CellPress
OPEN ACCESS

Trends in
Biotechnology

Review

Prime editing: advances and therapeutic applications

Zhihan Zhao [1,2], Peng Shang [1,2], Prarthana Mohanraju [1,2,*] and Niels Geijsen [1,2,*]

Clustered regularly interspaced short palindromic repeats-associated protein 9 (CRISPR–Cas)-mediated genome editing has revolutionized biomedical research and will likely change the therapeutic and diagnostic landscape. However, CRISPR–Cas9, which edits DNA by activating DNA double-strand break (DSB) repair pathways, is not always sufficient for gene therapy applications where precise mutation repair is required. Prime editing, the latest revolution in genome-editing technologies, can achieve any possible base substitution, insertion, or deletion without the requirement for DSBs. However, prime editing is still in its infancy, and further development is needed to improve editing efficiency and delivery strategies for therapeutic applications. We summarize latest developments in the optimization of prime editor (PE) variants with improved editing efficiency and precision. Moreover, we highlight some potential therapeutic applications.

Highlights

Prime editing is a 'search-and-replace' genome-editing technology that introduces all base-to-base conversions, as well as small insertions and deletions, without the need for double-strand breaks (DSBs) or donor DNA templates.

A major limitation of prime editing is its low editing efficiency. Several strategies have been developed to improve it by using an engineered prime-editing protein, improving the prime-editing guide RNA design, manipulating mismatch repair pathway, and optimizing the delivery strategy.

Continued refinement of prime editing will enable it to be safely and effectively implemented to treat a range of genetic disorders *ex vivo* and *in vivo*.

CRISPR–Cas-mediated precise genome editing

The simplicity and versatility of CRISPR–Cas systems has led to their rapid adoption as the most widely used genome-editing technology for site-specific DNA manipulations [1–3]. CRISPR–Cas-based tools typically consist of a nuclease that induces DNA **DSBs** (see Glossary) at a specific genomic locus targeted by a programmable guide RNA [4,5]. The DSBs are mostly resolved through one of the two major DSB repair pathways: non-homologous end joining (NHEJ) and **homology-directed repair (HDR)** [6–8]. Although NHEJ can efficiently religate two DSB ends, it is error-prone and generates insertions or deletions (indels) [9,10]. By contrast, HDR precisely introduces desired alterations including insertions, deletions, or substitutions based on a DNA repair template [11,12] (Figure 1A). However, HDR is restricted to the S/G2 phase of the cell cycle and is inefficient in most therapeutically relevant cell types [11,13]. Indeed, in most somatic cells, NHEJ outcompetes HDR in repairing the DSBs, resulting in a complex range of editing outcomes [5,14]. In addition, the generation of DSBs is associated with undesired editing outcomes such as large deletions [15], inversions [16], and translocations [15], and the initiation of cellular stress response mechanisms to preserve genome stability such as p53 activation [17–19]. To overcome this, HDR strategies that rely on single-strand breaks (SSBs) generated by CRISPR–**Cas9 nickase** (**nCas9**, D10A or H840A) [20] have been developed, albeit with low editing efficiency [21]. These challenges exemplify the need for the development of alternative precise genome-editing tools.

CRISPR–Cas-based **base editors (BEs)** can incorporate a desired modification without the requirement for a DSB, HDR, or donor DNA template, and can be applied in both dividing and non-dividing cells (Figure 1B) [22,23]. BEs are engineered fusion proteins consisting of a D10A nCas9 and a DNA deaminase domain that catalyzes the deamination of either cytidine (C) or adenosine (A) resulting in base conversions to thymine (T) or guanine (G), respectively (Figure 1B) [24,25]. As such, BEs are not universally applicable for 'fixing' disease-causing alleles that arise from specific insertions, deletions, or some base substitutions. Moreover, the editing efficiency and outcomes

[1]Leiden University Medical Center, Einthovenweg 20, 2300 RC Leiden, The Netherlands
[2]The Novo Nordisk Foundation Center for Stem Cell Medicine (reNEW), Leiden node, The Netherlands

*Correspondence:
p.mohanraju@lumc.nl (P. Mohanraju) and n.geijsen@lumc.nl (N. Geijsen).

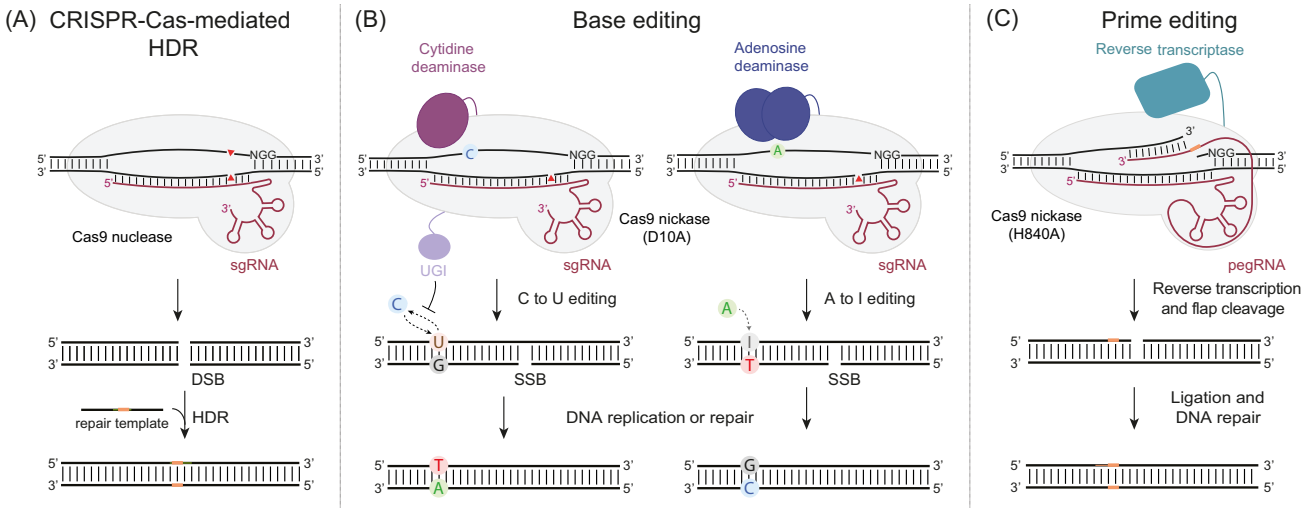

Figure 1. CRISPR–Cas-mediated precise genome-editing systems. (A) Cas9 nuclease is guided by a single guide RNA (sgRNA) to generate a targeted DNA double-strand break (DSB). In the presence of a repair template carrying the desired edits (orange), the cellular homology-directed repair (HDR) machinery repairs the DSB using the template, allowing precise incorporation of the template-carried edits in the genome. (B) Base editors (BEs) are engineered fusion proteins composed of nCas9 (D10A) and deaminase domain(s). Cytosine base editor (CBE) can convert C to U in a single strand. The resulting U:G heteroduplex can then be converted to a T:A base pair following DNA replication or repair. Another functional domain fused to the CBE, the uracil glycosylase inhibitor (UGI) domain, prevents U from reverting to C, thereby favoring C to T conversion. Adenine base editor (ABE) can deaminate A to form inosine (I) that has the same base-pairing preferences as G. Thus, the I:T heteroduplex can be converted to G:C following DNA replication and repair. For both ABE and CBE, nCas9 (D10A) nicks the target strand to create a SSB; the mismatch repair (MMR) machinery then pairs the deaminase-converted base with a properly matched base. Collectively, CBE and ABE can install all four transition mutations (C to T, T to C, A to G, and G to A). (C) Prime editor (PE) is an engineered fusion protein composed of nickase Cas9 (nCas9) and a reverse transcriptase (RT). The nCas9 creates an SSB on the non-target strand. The released 3′ end then hybridizes to the 3′ end of the prime-editing guide RNA (pegRNA) and is reverse transcribed by the RT domain. The reverse transcription incorporates the edits encoded in the pegRNA (orange) into the newly synthesized DNA strand. Equilibration between the edited 3′ flap and the unedited 5′ flap, endogenous 5′ flap cleavage and ligation, and DNA repair results in the stable incorporation of the desired edit in the genome. Abbreviation: CRISPR–Cas9, clustered regularly interspaced short palindromic repeats-associated protein 9.

of BEs can be affected by the sequence context of the target base. For example, the cytosine base editor (CBE) was more efficient when the target C was in the context of TC, and adenine base editor (ABE) was more efficient when the target A was in the context of YAC (Y is T or C) [24,25]. In addition, the target base must be in the activity window, where the positions are susceptible to deamination [24]. However, the presence of multiple editable bases within the BE activity window can result in undesired 'bystander' mutations [24–26].

Prime editing is the first precise genome-editing technology that allows all 12 possible base-to-base conversions, as well as insertions and deletions, that does not require DSBs or donor DNA [27]. Its broad editing spectrum potentially allows the correction of up to 89% of human genetic diseases [27]. PEs consist of a nCas9 (H840A) conjugated with an engineered reverse transcriptase (RT) paired with a **prime-editing guide RNA (pegRNA)** that both specifies the target site and encodes the desired edit (overview in Figure 1C and more details in Figure 2). In this review we describe the mechanism of prime editing, highlight various efforts to enhance its efficiency, and summarize some recent potential applications of prime editing in therapeutics.

Prime editing: basic mechanism and specificity

The PE protein is a fusion between a nCas9 (H840A) and an engineered Moloney murine leukemia virus reverse transcriptase (MMLV-RT). This nCas9–RT fusion protein combines with a pegRNA which comprises a spacer sequence that hybridizes to the target strand, the Cas9-

binding scaffold part of the guide RNA, and an RT template encoding the desired modification and a primer binding site (PBS) (Figure 2, step 1) [27]. The nCas9 of PE nicks the non-target strand to expose a 3′-single-stranded DNA (ssDNA) (Figure 2, step 1) that hybridizes to the PBS (Figure 2, step 2) allowing the associated RT to extend the nicked 3′-ssDNA using the RT template (Figure 2, step 3). The action of RT results in two redundant ssDNA flaps: a 5′ flap that contains the unedited sequence and a 3′ flap that contains the edited sequence (Figure 2, step 4). The fully complementary 5′ flap is thermodynamically favored to hybridize with the unedited strand. Nonetheless, the inherent susceptibility of 5′ flaps to excision by endogenous structure-specific endonucleases likely leads to hybridization of the edited 3′ flap, resulting in a heteroduplex. Finally, ligation and DNA mismatch repair (MMR) resolve heteroduplexes by copying information from the edited strand to the unedited strand, resulting in the permanent incorporation of the desired modification (Figure 2, step 5) [27].

In the first PE report [27], the authors made note of the remarkably low frequency of off-target prime editing and demonstrated that, in HEK293T cells, the average off-target prime-editing frequency of pegRNAs targeting *HEK3*, *HEK4*, *EMX1*, and *FANCF* at the top four known Cas9 off-target sites was <0.1%, <2.2 ± 5.2%, <0.1%, and <0.13 ± 0.11%, respectively. By comparison, off-target editing with traditional Cas9-sgRNA was 16 ± 16%, 60 ± 26%, 48 ± 28%, and 4.3 ± 5.6%, respectively. The low off-targeting frequency of prime editing was confirmed in subsequent independent studies in a variety of model organisms such as mouse embryos (<0.1%) [28–31], organoid lines (no observable off-target mutations) [32,33], and plants (0.00–0.23%) [34]. The high specificity of the prime-editing system is likely due to the additional two-step DNA hybridization of the target DNA–PBS and target DNA–RT template required by PE leading to low hybridization and editing at off-target loci [27]. Nonetheless, reverse transcription of 3′-extended pegRNAs can proceed into the guide scaffold, resulting in scaffold sequence insertion at the target locus. Indeed, although the frequency of such events was low, unwanted pegRNA-mediated scaffold insertions were demonstrated in both HEK293T cells and zebrafish [27,35]. The promiscuous activity of deaminase domains in BEs was shown to sometimes lead to Cas9-independent off-target editing in both DNA and RNA [36–38]. Similarly, broad overexpression of RT in the nucleus may also lead to PE-independent off-target reverse transcription and genome editing. However, no significant genome-wide or transcriptome-wide PE-independent off-target mutations or perturbations have been observed [27,39,40].

Overcoming current challenges in using PE

PE has been demonstrated to allow specific gene modification in various cell types [27,28,35,41–44], organoids [32,33], zebrafish [35], *Drosophila* [39], mice [29,45–48], and plants [49–53]. However, the technology is still in its infancy and needs to overcome several limitations to realize its full potential. In particular, the low editing efficiency remains a crucial challenge. The results of an experimental analysis of PE editing efficiency on thousands of tested sites using a lentiviral second-generation PE (PE2) showed that the editing efficiency of PE2 is typically below 20% in immortalized cell lines and drops even further in primary cells [54]. Moreover, the editing efficiency greatly varies across target loci and cell types, hampering its broad application [27]. In addition to the efficiency of the PE itself, effective delivery of prime-editing systems into the target cells also remains a challenge (Box 1). The size of full-length PE precludes its incorporation into a single adeno-associated virus (AAV) vector system, conferring a considerable challenge to its safe *in vivo* delivery. Thus, approaches to enhance the efficiency and fidelity of PE in different cell types and to survey potential undesired consequences of PE in different cell lines need to be developed. Moreover, novel delivery technologies need to be developed for the successful deployment of PE in therapeutics. We discuss below some of the emerging strategies to address these limitations.

Glossary

Base editors (BEs): the basis of a genome-editing technology that uses Cas9 nickase together with a base-modifying enzyme that can either convert cytosine to thymine or adenine to guanine, thereby inducing targeted mutations without introducing DSBs.
Cas9 nickase (nCas9): a Cas9 variant developed by mutating one of the two endonuclease domains resulting in its inability to generate DSBs, thereby generating a nick in the target DNA. Frequently used examples are SpCas9-D10A and SpCas9-H840A which cut the target strand and non-target strand, respectively. In SpCas9, the D10A mutation inactivates the RuvC nuclease domain whereas the H840A mutation inactivates the histidine/asparagine (HNH) endonuclease domain.
Double-strand DNA break (DSB): cleavage of DNA such that the backbones of both strands are cleaved simultaneously. Targeting by conventional CRISPR–Cas nucleases generates DSBs which then stimulate endogenous DNA repair pathways to repair the targeted sequence.
Homology-directed repair (HDR): a precise repair mechanism that uses donor DNA to accurately correct a DNA break. The donor DNA must include homology to the two flanking DNA ends.
Prime editing: a genome-editing technology that allows precise engineering of targeted insertions, deletions, and base substitutions. It utilizes a Cas9 nickase (H840A) fused to a reverse transcriptase (RT) domain and a modified sgRNA, known as the pegRNA that serves as a template for the RT and encodes the desired genetic modification. The Cas9–RT fusion is called the prime editor (PE).
Prime-editing guide RNA (pegRNA): a guide RNA that serves the dual purpose of guiding the PE protein to the targeted locus and encoding the desired edit. It is a modified sgRNA with a 3′ extension composed of a primer binding site (PBS) that hybridizes to the 3′ end of the nicked strand and an RT template encoding the desired edit and downstream genomic sequence.
Protospacer adjacent motif (PAM): a short (2–8 nt) conserved sequence adjacent to the DNA target sequence that is required for target recognition and cleavage by DNA-targeting CRISPR–Cas nucleases.

Improving the PE protein

The first-generation PE (PE1) uses the wild-type MMLV RT fused to the C terminus of nCas9 (H840A) (Figure 3A) [27]. This resulted in 0.7–5.5% base substitution efficiency. Engineering of five specific mutations (D200N, L603W, and T330P to improve thermostability; T306K and W313F to enhance binding of RT to the pegRNA) [55] in the MMLV RT domain yielded PE2 (Figure 3A) with a 5.1-fold increase in base substitution efficiency over the PE1 [27]. The addition of an N-terminal c-Myc nuclear localization signal (NLS) and inclusion of both a variant bipartite SV40 NLS (vBP-SV40) and a SV40 NLS at the C terminus of PE (PE*) (Figure 3A) results in its nearly complete nuclear localization, improving overall base substitution efficiency by 1.9-fold over PE2 [48]. Combining a human codon-optimized RT, an additional C-terminal c-Myc NLS, and activity-improving mutations in nCas9 results in a more efficient PE variant (PEmax) (Figure 3A). PEmax exhibits a 2.5-fold and 1.2-fold increase in base substitution efficiency compared to PE2 in HeLa and HEK293T cells, respectively [56].

Single guide RNA (sgRNA): a synthetic chimera that contains the CRISPR RNA (crRNA) fused to the transactivating RNA (tracrRNA) using a tetraloop.

The fusion of additional functional domains to PE has also been employed to augment the editing efficiency. Addition of a of Rad51 DNA-binding domain between the nCas9 and RT domains, named hyPE2 (Figure 3A), increases PE2 efficiency by a median of 1.4- and 1.5-fold in HEK293T and HCT116 cells, respectively [44]. The improvement was notably high when using a PBS with low melting temperature (T_m), suggesting that Rad51 presumably facilitates the binding of the PBS to the 3′-ssDNA generated by the nCas9 nick, thereby enhancing reverse transcription [44]. Moreover, fusion of chromatin-modulating peptides to PE3 (where an additional guide RNA is added to the PE2 system to nick the unedited strand, details below), named

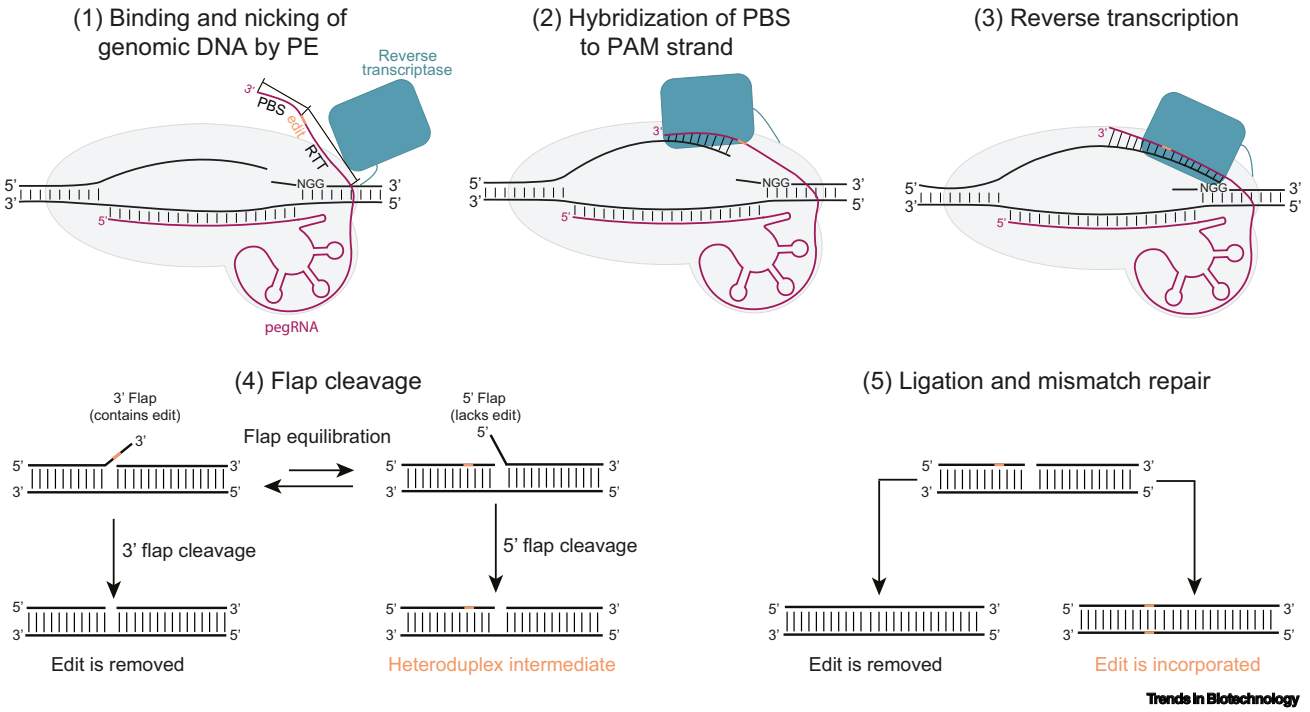

Figure 2. Mechanism of prime editing. Illustration detailing the putative steps of the prime-editing system. (1) Cas9 nickase is guided to the target by the prime-editing guide RNA (pegRNA) and generates a nick on the non-target strand, exposing a 3′-hydroxyl group. (2) The resulting 3′ end hybridizes to the primer binding site (PBS) and (3) primes the reverse transcriptase to synthesize DNA using the sequence containing the desired edit encoded in the reverse transcription template (RTT) of the pegRNA. (4) The newly synthesized strand leads to an equilibration between the intermediates with 3′ flap containing the desired edit and 5′ flap that does not contain the desired edit. The 5′ flap is degraded by cellular enzymes. The edited 3′ flap is ligated into the genome. (5) Finally, repair of the complementary genomic DNA strand using the edited strand as the template by DNA repair or replication results in stable installation of the edit. Abbreviations: PAM, protospacer adjacent motif; PE, prime editor.

Box 1. CRISPR delivery systems

Gene-editing agents can be delivered into cells as DNA or mRNA, or directly as protein and ribonucleoprotein complexes (RNPs) [94]. In general, delivery techniques can be divided into viral and non-viral delivery [95]. Viral vectors, especially adeno-associated virus (AAV), can deliver nucleic acid cargos to many cells and have shown great promise in clinical trials because of their efficient cellular uptake, high biocompatibility, and multiple serotype specificities [78]. However, AAV packaging capacity is limited and prolonged expression leads to increased off-targeting frequency [96,97]. Non-viral delivery vectors include electroporation [98], lipid-mediated transfection [99], nanoparticles [100], cell-penetrating peptide [101], hydrodynamic delivery [102], microinjection [103], induced transduction by osmocytosis and propanebetaine (iTOP) [92], and virus-like particles (VLPs) [104] that can transiently deliver RNP-based gene-editing agents, thereby reducing off-target editing. From a safety perspective, RNP delivery vehicles are the most attractive, and the development of improved RNP delivery vehicles will be highly impactful for future therapeutic applications [94].

CMP-PE3-V1, improves chromatin accessibility, resulting in a 2.55- and 3.92-fold higher targeting efficiency than PE3 at *Igf2* and *Adamts20* loci in the mouse cell lines (Figure 3A) [28]. Likewise, fusion of a dual DNA repair-related peptide, IGFpm1-NFATC2IPp1, to a PE (IN-PE2) leads to a median 1.63-, 1.31-, and 1.23-fold increase in prime editing across dozens of target sites in mESC, HEK293T, and U2OS cells, respectively (Figure 3A) [57]. Interestingly, this peptide fusion is unlikely to function through interactions with MMR machinery, and instead increases cellular protein expression of the PE. Consequently, the resulting high levels of PE in the cell increase the overall prime-editing efficiency. More recently, based on a previously reported plant PE (PPE) [50], authors from the same laboratory constructed an enhanced PPE (ePPE) in which a viral nucleocapsid protein that has nucleic acid chaperone activity is inserted between the nCas9 and the RNase H domain-deleted MMLV-RT (Figure 3A). In plant cells, this ePPE achieves a 1.8–3.4-fold improvement in prime-editing efficiency compared with PPE [58].

Optimizing the pegRNA

Although the programmability of prime editing allows straightforward editing, defining a suitable pegRNA design necessitates thorough optimization. The lengths of the PBS and RT template significantly affect PE efficiency [27]. Therefore, different pegRNAs with varying PBS and RT template lengths must be tested for any given target site. Typically, the PBS and RT template are in the ranges of 8–15 nt and 10–20 nt, respectively [27]. Several computational tools to aid in optimal pegRNA design have been developed, such as pegFinder [59], PrimeDesign [60], PE-Designer [61], PnB Designer [62], and pegIT [63].

Given that the PBS is complementary to part of the spacer at the 5′ end of pegRNA, their annealing could cause pegRNA circularization, potentially hampering editing. To inhibit circularization, a 20-nt hairpin forming a Csy4 recognition site was fused to the 3′ end of canonical pegRNA [64]. Moreover, combining coexpression of the sgRNA and pegRNA in a single transcript to optimize their stoichiometry for the PE3 system, and mutating the fourth uracil of consecutive uracils in the scaffold of pegRNA into a cytosine to eliminate a putative transcription termination signal, led to higher pegRNA expression. This system, called enhanced PE (ePE), results in a 1.9-fold increase in base substitution efficiency over PE3 without increasing indels [64]. Furthermore, to stabilize the secondary structure of pegRNA, a non-C/G pair was changed to a C/G pair in the small hairpin (apegRNA), resulting in higher frequencies of targeted insertions and deletions compared to regular pegRNA [65]. The incorporation of structured RNA motifs such as an exoribonuclease-resistant RNA motif (xrRNA) or a trimmed prequeosine$_1$-1 riboswitch aptamer (tevopre Q1) to the 3′ terminus of pegRNA can enhance their stability and prevent degradation by cellular exonucleases, resulting in 2.5–4.5-fold improved prime-editing outcomes compared to a regular pegRNA in a variety of cell types (Figure 3B) [66,67]. Hence, the use of engineered pegRNAs will likely reduce the need for exhaustive screening and can substantially advance the application scope of prime editing.

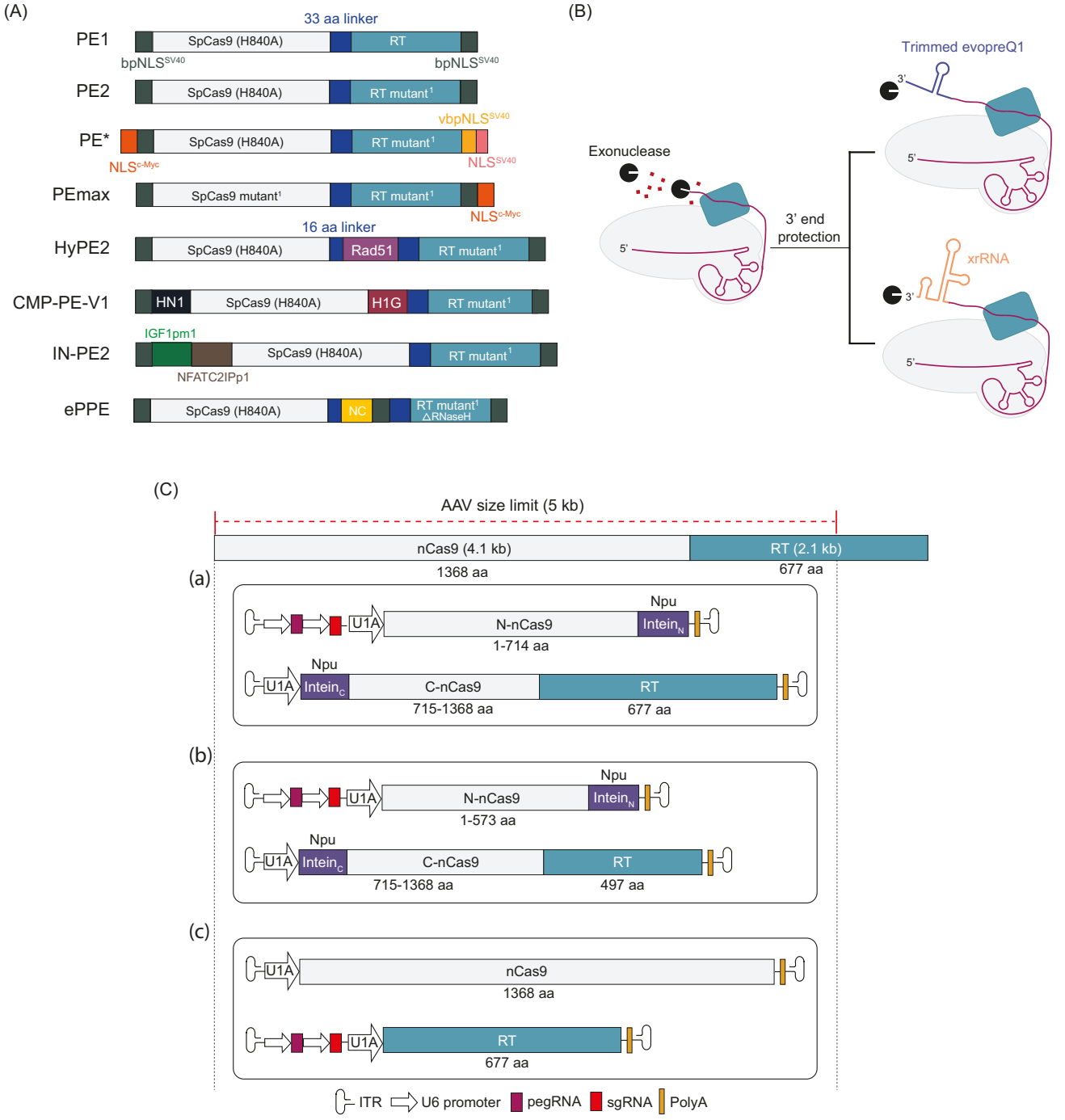

Trends in Biotechnology

(See figure legend at the bottom of the next page.)

Manipulating cellular DNA repair pathways

The overall prime-editing efficiency depends on the ability to strongly favor the incorporation of a desired edit. In PE3, this can be achieved by using an extra **single guide RNA (sgRNA)** that introduces a nick in the unedited strand distal to the edit site, which likely triggers the intrinsic DNA repair response that favors the editing outcome [27]. PE3 results in 1.5–4.2-fold increase in base substitution efficiency over PE2 in HEK293T cells. Further improvement of this system, called PE3b, also uses a nicking sgRNA but only targets the edited sequence, resulting in 13-fold decreased levels of indel products by preventing nicking of the non-edited DNA strand until the other strand is converted to the edited sequence [27]. Akin to PE3, nuclease-based PE (PEn) outperforms nickase-based PE at hard-to-edit targets by introducing a nick in the unedited strand, thus directing the DNA repair response towards the edited outcome. PEn exhibits a 2–3-fold higher insertion and base substitution over PE3 [42]. In addition, the introduction of silent mutations at appropriate positions in the reverse transcription template (RTT; spegRNA) enhances the intended base substitution efficiency by an average of 353-fold compared to regular pegRNA in PE3 [65]. Moreover, the apegRNA and the mutations underlying spegRNA can be combined (aspegRNA) to further enhance PE editing efficiency in human cells [65]. Using paired pegRNAs to encode the same edits in both DNA strands can improve editing efficiency in human cells and rice protoplasts [53]. Nevertheless, this paired-pegRNA strategy seems to perturb genomic integrity by promoting large DNA fragment deletions (1–10 kb), integration (>5 kb), and inversion (40 kb) [68–72].

The cellular factors and pathways involved in the 3′ flap cleavage have not been well established, but MMR (Box 2) activity strongly impedes the efficiency and homogeny of prime-editing outcomes [56,73]. Inhibiting key MMR factors such as MLH1 and MSH2 using an engineered MMR-inhibiting protein (MLH1dn) indeed increased PE efficiency [56,73]. The PE4 (PE2+MLH1dn) and PE5 (PE3+MLH1dn) systems include transient expression of MLH1dn, which enhances the efficiency of different prime edits by an average 7.7-fold and twofold compared to PE2 and PE3, respectively. Moreover, strategic installation of synonymous mutations near the intended edit site also enhances prime-editing outcomes by evading MMR recognition, even without MLH1dn [56].

Increasing targeting scope

Conventional PEs are limited in their target scope due to the restraints imposed by the **protospacer adjacent motif (PAM)** sequence of the *Streptococcus pyogenes* Cas9 (SpCas9). Previously developed SpCas9 PAM variants have been successfully integrated into PEs to relax the canonical PAM preferences [74–76]. Three engineered PEs extend the target scope without sacrificing editing efficiency: PE-SpG (PAM:5'-NG, N is any nucleotide), PE-NG (PAM:5'-NG), and PE-SpRY (PAM-independent) [77]. Notably, the PE-SpRY variant extends the coverage of human genetic diseases to 94.4% and increases the number of PE3b applicable sites for improved editing efficiency without introducing more indels [77]. The PE3b-SpRY variant

Figure 3. Strategies to improve the efficiency of prime editing. (A) Optimizing the prime editor (PE) protein. Schematic architectures of PE1, PE2, PE*, PEmax, HyPE2, CMP-PE-V1, IN-PE2 editors, and ePPE. The reverse transcriptase (RT) mutant[1] comprises MMLV RT with five mutations (D200N, T306K, W313F, T330P and L603W). The SpCas9 mutant[1] comprises SpCas9 with three mutations (R221K, N394K, and H840A). Rad51 is a single-stranded DNA-binding protein domain, HN1 is high mobility group nucleosome-binding domain 1, and H1G is the histone H1 central globular domain. IGF1pm1 (I) and NFATC2IPp1 (N) are two peptides derived from DNA repair proteins. NC is a viral nucleocapsid protein. (B) Stabilization of the prime-editing guide RNA (pegRNA). Addition of the structured RNA motifs (trimmed evopre Q1 and xrRNA) to the 3′ terminus of pegRNA protects the 3′ extension from degradation by exonucleases. evopreQ1 is a modified prequeosine$_1$-1 riboswitch aptamer and xrRNA is an exoribonuclease-resistant RNA motif. (C) Current strategies for *in vivo* delivery. Schematic of a split-intein dual AAV PE. Full-length PE2 (a) or PE2 with truncated RT (b) was reconstituted from two PE2 fragments (N-nCas9 and C-nCas9-RT) employing the Npu DnaE split intein. (c) nCas9 and MMLV RT were subcloned into two separate AAV8 vectors without inteins. Abbreviations: AAV, adeno-associated virus; C, carboxy-terminal; DnaE: α subunit of DNA polymerase III; ITR: inverted terminal repeat; MMLV, Moloney murine leukemia virus; N, amino-terminal; *Npu*, *Nostoc punctiforme*.

Box 2. DNA mismatch repair (MMR)

DNA MMR is a highly conserved pathway from prokaryotes to eukaryotes that plays a key role in maintaining genomic integrity [105]. It repairs base mismatches and small insertions or deletions caused by misincorporation errors during DNA replication [106]. In eukaryotes, the nicked strand is replaced by MMR that resolves DNA heteroduplexes containing mismatches [106,107]. During this process, MutS, MutL, exonuclease, polymerase, and ligase are involved [56,108]. First, MutSα (MSH2–MSH6) or MutSβ (MSH2–MSH3) binds to the heteroduplex to recognize mismatches and initiate MMR [109,110]. MutLα, recruited by MSH2, then cuts the strand that contains the nick [111,112]. Finally, exonuclease 1, a 5′–3′ exonuclease, excises the heteroduplex, the polymerase then synthesizes the excised DNA strand, and the ligase seals the nascent stand [113,114]. Thus, in prime editing the strand containing the desired edits is preferentially removed. Identifying ways to inhibit this process can significantly improve editing outcomes [56].

has been used to introduce the clinically significant BRAF V600E mutation with an editing efficiency of 11.8%, which was not possible using conventional PEs [77].

Developing PE delivery strategies

Most *in vivo* studies are now based on AAV delivery owing to its efficient cellular uptake, low immunogenicity, and range of serotype specificities [78]. However, PE exceeds the cargo capacity of a single AAV vector, making safe and efficient delivery challenging. To counteract this, split inteins that can reassemble two split PE (sPE) parts into the full-length protein have been applied for PE delivery *in vivo* in mouse liver and retina. One such variant consists of the PE split into two parts at Ser714. Dual AAV8s were used to deliver the split inteins (sPE714) into mouse liver to correct the E342K mutations in SERPINA1. A 3.1% ± 0.6% correction rate after 10 weeks was observed (Figure 3C) [48]. Another study tested several split sites (Thr994, Ser1005, Ser1024, and Thr1032 in nCas9) and revealed that sPE1024 performed best to edit *Dnmt1* in mouse retina, paving the way for *in vivo* gene-editing therapy using PE [79]. In addition, a compact PE (cPE) was created by removing the RNase H domain of RT (Figure 3C). cPE can efficiently induce precise editing *in vivo* with an efficiency similar to the full-length PE. After testing several split sites, split-cPE2-573 was delivered via dual-AAV8 into mouse liver to edit *Pcsk9* with 13.5% editing efficiency after 4 weeks [45]. Interestingly, an sPE, in which the nCas9 is not tethered to the RT, was delivered using two AAV8 vectors (one expressing nCas9, and another expressing the RT, the pegRNA, and a nicking sgRNA) (Figure 3C) [80]. This sPE variant corrected 1.3% of A-to-G mutations in a mouse model of type I tyrosinemia. In addition to the viral delivery methods described above, electroporation of a PE2 ribonucleoprotein complex (RNP) into zebrafish zygotes was shown to yield a 30% editing efficiency in somatic cells and even resulted in germline transmission [35]. As such, mRNA- or RNP-based delivery systems may help to overcome the size restrictions imposed by viral vectors and provide attractive and safe means for the application of PE systems in target cells.

Overall, prime editing represents a promising strategy for precise genome editing with remarkable flexibility and reliability. Recent efforts to improve the efficiency, editing scope, and delivery of prime editing have resulted in more rapid uptake of the technology, especially in the context of biotechnological and pharmacological applications, as we discuss in the next section.

Prime editing in therapeutic applications

In vivo gene editing to treat patients with genetic diseases is a longstanding goal of modern medicine. Given that prime editing has some considerable strengths over other CRISPR–Cas9-mediated genome-editing methods, it has been rapidly deployed *in vivo* and its potential to treat several genetic disorders has been examined [81]. Although PEs have not yet reached clinical trials, a few proof-of-principle studies using mammalian animal models provide a foundation for future clinical trials. We highlight here several recent examples in which PE use may eventually lead to new clinical solutions (Table 1).

First, PE3 has been used to insert 2 nt into exon 52 of the ΔEx51 iPSC model, the most common single-exon deletion mutations in Duchenne muscular dystrophy (DMD) patients, with an efficiency of 54% [82]. Isolation and differentiation of these prime-edited iPSCs into cardiomyocytes resolved the contractile abnormalities that were observed in unedited cells. In addition, subretinal injection of split AAV-PE2 in rd12 mice, a mouse model of human Leber congenital amaurosis (LCA) in which a nonsense mutation is produced by a C to T change in exon 3 of *RPE65*, showed an average editing efficiency of 28% without any unintended edits. Moreover, the AAV-PE2-treated rd12 mice revealed more light-induced electrical responses compared to control mice [83]. By contrast, in the same mouse model, the correction efficiency of Cas9-mediated HDR was only 1.2% ± 0.3% with an indel frequency of 17% ± 8%; and the correction efficiency for base editor was 11% ± 7% with substantial 7.7% ± 5% frequencies of bystander edits, demonstrating the advantage of the PE system over other precise genome-editing methods in both editing efficiency and editing-outcome homogeneity [83].

PEs have also been applied in three mouse models of liver diseases. The $Fah^{mut/mut}$ mouse model of tyrosinemia type I is caused by a G-to-A inactivating mutation in the fumarylacetoacetate hydrolase (*Fah*) gene. Hydrodynamic injection of PE3-related plasmids into $Fah^{mut/mut}$ mice yielded an average editing efficiency of 11.5% [83]. Moreover, all PE3-edited mice survived until the end of the experiment (40 days), whereas mice injected with phosphate-buffered saline showed substantial weight loss and died before 30 days [83]. PE was also applied in a PiZ transgenic mouse model of α1 antitrypsin deficiency (AATD), caused by an inactivating G-to-A mutation in the serpin peptidase inhibitor family a member 1 (*SERPINA1*) gene. Hydrodynamic injection of a plasmid encoding NLS-optimized PE2 (PE2*)

Table 1. Key examples of preclinical gene and cell therapy applications of prime editing

Disease model	Key organ (cell type)	PE variant	Prime-editing strategy	Delivery vehicle/method	Editing outcomes	Refs
Duchenne muscular dystrophy (DMD) in a human ΔEx51 iPSC model	iPSCs	PE3	GT insertion in exon 52 of *DMD*	Electroporation	Successful restoration of dystrophin protein expression was demonstrated in prime-edited iPSC-derived cardiomyocytes The arrhythmic defect was alleviated in prime-edited iPSC-derived cardiomyocytes	[82]
Leber congenital amaurosis in *rd12* mice	Retina	PE2	T to C transition in exon 3 of *Rpe65*	Triple AAV2 vectors	Distinct membrane and cytoplasmic expression of RPE65 protein in RPE tissue was observed in the edited mice The edited mice had better dark-adapted light-induced electrical responses	[83]
Tyrosinemia type I in $Fah^{mut/mut}$ mice	Liver	PE3	A to G transition in exon 8 of *Fah*	Hydrodynamics-mediated non-viral vector delivery	The edited mice showed an average of 61% FAH^+ cells in the liver at day 40 The edited mice exhibited lower weight loss and survived at day 40	[83]
α1-Antitrypsin deficiency (AATD) in mice	Liver	PE2*	A to G transition in exon 5 of *Serpina1*	Hydrodynamic-mediated non-viral vector delivery	6.7% gene correction with 2.7% indels at day 45	[48]
		PE3		Dual AAV8 vectors	3.1% gene correction with 0.4% indels at day 70	
Phenylketonuria in Pah^{enu2} mice	Liver	$PE3^{\Delta RnH}$ (variant with the RT lacking the RNase H domain)	C to T transition in exon 7 of *Pah*	Dual AAV8 vectors	<2% gene correction	[47]
				Human adenoviral vector 5 (HAdV5)	11.1% gene correction with <0.2% indels L-Phe concentrations were reduced to therapeutically satisfactory levels of 100 ± 34 μM	

(Figure 3A) into mouse liver increased A-to-G correction in PiZ *SERPINA1* (6.7% on average) by 3.1-fold compared to PE2 (2.1%) [48]. Finally, PE was used in a *Pah*^{enu2} mouse model of phenylketonuria (PKU) caused by inactivating the phenylalanine hydroxylase (*Pah*) gene with a T-to-C mutation, resulting in abnormally high blood L-Phe concentrations [84]. Human adenoviral vector 5 (AdV) was used to deliver PE3$^{\Delta RnH}$ (in which the RNase H domain of RT in PE protein was deleted) to the *Pah*^{enu2} mouse model. The average correction efficiencies of 11.1% (up to 17.4%) in neonates, leading to therapeutic reduction of blood phenylalanine, without inducing detectable off-target mutations or prolonged liver inflammation, demonstrating the potential role of PE in the clinical treatment of PKU [47].

Taken together, these examples highlight that PE systems have the potential to correct monogenic diseases caused by a variety of mutations. In addition, PE allows the introduction of multiple simultaneous edits using tandem arrays of pegRNAs [85–87]. This makes it a valuable tool for treating polygenic diseases, for example, coronary artery disease. Moreover, using paired pegRNAs allows the insertion of large DNA fragments (>100 bp), making the correction of multiple gene variants located in a hotspot possible [69]. However, the efficiency of PE systems remains relatively low, even using more recent augmented versions of the system. Furthermore, the large size of PE effectors makes therapeutic delivery of these systems a challenge. Finally, additional work will be necessary to assess its long-term safety. Combined, these concerns may restrain PE from being applied directly in humans in the near future. Further optimization of PE editing efficiency, taking advantage of advanced whole-genome next-generation sequencing technologies and new delivery strategies, the *ex vivo* applications of prime editing may first bring its benefits to cancer or blood disease therapies.

Concluding remarks and future perspectives

The progression from the initial discovery and characterization of the prime-editing system to potential applications in biomedical sciences has occurred at a breathtaking pace. The improved flexibility and specificity of prime editing over other CRISPR–Cas9-mediated genome-editing strategies has made the use of PE highly attractive. However, there are several issues that need to be addressed, most importantly the issue of low efficiency. To further enhance the efficiency of prime editing, the structure of the PE–pegRNA–DNA complex needs to be elucidated (see Outstanding questions). Further optimization of the PE effector could be achieved by exploiting more active nCas9 or RT variants by rational modification, *in vitro* evolution approaches, and fusion with additional or combinatorial functional protein domains. In the absence of further improvements of PE efficiency, therapeutic application of PE systems may be limited to disorders that require minimal functional restoration of the corrected genes, or to situations where more than the typical two autosomal copies of a gene are present, increasing the likelihood of functional gene correction. For example, this is the case in p47^{phox}-deficient chronic granulomatous disease, where the *NCF1* gene is inactivated by the transfer of a ΔGT (75_76delGT) mutation from one of the two processed pseudogenes, resulting in a nonsense mutation that prevents translation into functional protein. In the context of this defect, correction of either the *NCF1* gene itself or of any of the processed pseudogenes will correct the disorder, thus increasing the likelihood of functional therapeutic benefit [88]. Other examples include genetic skeletal muscle disorders and some metabolic disorders. Because skeletal muscle fibers are syncytia, containing thousands of nuclei per cell, this elevates the chance of gene correction per cell. However, a question of course remains concerning what level of gene correction is needed on a per-cell basis to have functional therapeutic benefit. In addition, the *in vivo* delivery of large PE systems in combination with pegRNA remains a substantial hurdle. To this end, the development of new viral vectors [89], nanoparticle vectors [90,91], and RNP- or mRNA- based delivery approaches [28–30,92,93] becomes urgent (see Outstanding questions). In addition, we need to

Outstanding questions

The exact mechanistic details of the prime editing are not fully understood. Can the structures of various PE variants aid in understanding how the efficiency of prime editing can be improved?

What DNA repair mechanisms are involved in prime editing?

How can the large prime-editing complex efficiently and safely be delivered in a therapeutic setting?

better understand how cell state and/or cell type influence prime-editing efficiency, and how different DNA repair mechanisms result in productive or unproductive prime editing (see Outstanding questions). Collectively, these developments have the potential to improve the performance of PE, and we expect that the number and diversity of PE applications, including *in vivo*, will continue to grow.

Declaration of interests

The authors declare no conflicts of interest.

References

1. Adli, M. (2018) The CRISPR tool kit for genome editing and beyond. *Nat. Commun.* 9, 1911
2. Moon, S.B. *et al.* (2019) Recent advances in the CRISPR genome editing tool set. *Exp. Mol. Med.* 51, 1–11
3. Hsu, P.D. *et al.* (2014) Development and applications of CRISPR–Cas9 for genome engineering. *Cell* 157, 1262–1278
4. Jinek, M. *et al.* (2012) A programmable dual-RNA-guided DNA endonuclease in adaptive bacterial immunity. *Science* 337, 816–821
5. Cong, L. *et al.* (2013) Multiplex genome engineering using CRISPR/Cas systems. *Science* 339, 819–823
6. Liang, F. *et al.* (1998) Homology-directed repair is a major double-strand break repair pathway in mammalian cells. *Proc. Natl. Acad. Sci. U. S. A.* 95, 5172–5177
7. Jeggo, P. (1998) DNA breakage and repair. *Adv. Genet.* 38, 185–218
8. Ceccaldi, R. *et al.* (2016) Repair pathway choices and consequences at the double-strand break. *Trends Cell Biol.* 26, 52–64
9. Lieber, M.R. (2010) The mechanism of double-strand DNA break repair by the nonhomologous DNA end joining pathway. *Annu. Rev. Biochem.* 79, 181–211
10. Chiruvella, K.K. *et al.* (2013) Repair of double-strand breaks by end joining. *Cold Spring Harb. Perspect. Biol.* 5, a012757
11. Heyer, W.-D. *et al.* (2010) Regulation of homologous recombination in eukaryotes. *Annu. Rev. Genet.* 44, 113–139
12. Yeh, C.D. *et al.* (2019) Advances in genome editing through control of DNA repair pathways. *Nat. Cell Biol.* 21, 1468–1478
13. Lin, S. *et al.* (2014) Enhanced homology-directed human genome engineering by controlled timing of CRISPR/Cas9 delivery. *eLife* 3, e04766
14. Mali, P. *et al.* (2013) RNA-guided human genome engineering via Cas9. *Science* 339, 823–826
15. Kosicki, M. *et al.* (2018) Repair of double-strand breaks induced by CRISPR–Cas9 leads to large deletions and complex rearrangements. *Nat. Biotechnol.* 36, 765–771
16. Mani, R.S. and Chinnaiyan, A.M. (2010) Triggers for genomic rearrangements: insights into genomic, cellular and environmental influences. *Nat. Rev. Genet.* 11, 819–829
17. Ihry, R.J. *et al.* (2018) p53 inhibits CRISPR–Cas9 engineering in human pluripotent stem cells. *Nat. Med.* 24, 939–946
18. Enache, O.M. *et al.* (2020) Cas9 activates the p53 pathway and selects for p53-inactivating mutations. *Nat. Genet.* 52, 662–668
19. Haapaniemi, E. *et al.* (2018) CRISPR–Cas9 genome editing induces a p53-mediated DNA damage response. *Nat. Med.* 24, 927–930
20. Nishimasu, H. *et al.* (2014) Crystal structure of Cas9 in complex with guide RNA and target DNA. *Cell* 156, 935–949
21. Davis, L. and Maizels, N. (2014) Homology-directed repair of DNA nicks via pathways distinct from canonical double-strand break repair. *Proc. Natl. Acad. Sci. U. S. A.* 111, E924–E932
22. Porto, E.M. *et al.* (2020) Base editing: advances and therapeutic opportunities. *Nat. Rev. Drug Discov.* 19, 839–859
23. Anzalone, A.V. *et al.* (2020) Genome editing with CRISPR–Cas nucleases, base editors, transposases and prime editors. *Nat. Biotechnol.* 38, 824–844
24. Komor, A.C. *et al.* (2016) Programmable editing of a target base in genomic DNA without double-stranded DNA cleavage. *Nature* 533, 420–424
25. Gaudelli, N.M. *et al.* (2017) Programmable base editing of A*T to G*C in genomic DNA without DNA cleavage. *Nature* 551, 464–471
26. Gehrke, J.M. *et al.* (2018) An APOBEC3A–Cas9 base editor with minimized bystander and off-target activities. *Nat. Biotechnol.* 36, 977–982
27. Anzalone, A.V. *et al.* (2019) Search-and-replace genome editing without double-strand breaks or donor DNA. *Nature* 576, 149–157
28. Park, S.J. *et al.* (2021) Targeted mutagenesis in mouse cells and embryos using an enhanced prime editor. *Genome Biol.* 22, 170
29. Liu, Y. *et al.* (2020) Efficient generation of mouse models with the prime editing system. *Cell Discov.* 6, 27
30. Lin, J. *et al.* (2021) Modeling a cataract disorder in mice with prime editing. *Mol. Ther. Nucleic Acids* 25, 494–501
31. Gao, P. *et al.* (2021) Prime editing in mice reveals the essentiality of a single base in driving tissue-specific gene expression. *Genome Biol.* 22, 83
32. Schene, I.F. *et al.* (2020) Prime editing for functional repair in patient-derived disease models. *Nat. Commun.* 11, 5352
33. Geurts, M.H. *et al.* (2021) Evaluating CRISPR-based prime editing for cancer modeling and CFTR repair in organoids. *Life Sci. Alliance* 4, e202000940
34. Jin, S. *et al.* (2021) Genome-wide specificity of prime editors in plants. *Nat. Biotechnol.* 39, 1292–1299
35. Petri, K. *et al.* (2022) CRISPR prime editing with ribonucleoprotein complexes in zebrafish and primary human cells. *Nat. Biotechnol.* 40, 189–193
36. Doman, J.L. *et al.* (2020) Evaluation and minimization of Cas9-independent off-target DNA editing by cytosine base editors. *Nat. Biotechnol.* 38, 620–628
37. Grünewald, J. *et al.* (2019) Transcriptome-wide off-target RNA editing induced by CRISPR-guided DNA base editors. *Nature* 569, 433–437
38. Fan, J. *et al.* (2021) Cytosine and adenine deaminase base-editors induce broad and nonspecific changes in gene expression and splicing. *Commun. Biol.* 4, 882
39. Bosch, J.A. *et al.* (2021) Precise genome engineering in *Drosophila* using prime editing. *Proc. Natl. Acad. Sci. U. S. A.* 118, e2021996118
40. Kim, D.Y. *et al.* (2020) Unbiased investigation of specificities of prime editing systems in human cells. *Nucleic Acids Res.* 48, 10576–10589
41. Habib, O. *et al.* (2022) Comprehensive analysis of prime editing outcomes in human embryonic stem cells. *Nucleic Acids Res.* 50, 1187–1197
42. Adikusuma, F. *et al.* (2021) Optimized nickase- and nuclease-based prime editing in human and mouse cells. *Nucleic Acids Res.* 49, 10785–10795
43. Surun, D. *et al.* (2020) Efficient generation and correction of mutations in human iPS cells utilizing mRNAs of CRISPR base editors and prime editors. *Genes (Basel)* 11, 511
44. Song, M. *et al.* (2021) Generation of a more efficient prime editor 2 by addition of the Rad51 DNA-binding domain. *Nat. Commun.* 12, 5617
45. Zheng, C. *et al.* (2022) A flexible split prime editor using truncated reverse transcriptase improves dual-AAV delivery in mouse liver. *Mol. Ther.* 30, 1343–1351
46. Aida, T. *et al.* (2020) Prime editing primarily induces undesired outcomes in mice. *bioRxiv* Published online August 6, 2020. https://doi.org/10.1101/2020.08.06.239723

47. Böck, D. *et al.* (2022) In vivo prime editing of a metabolic liver disease in mice. *Sci. Transl. Med.* 14, eabl9238
48. Liu, P. *et al.* (2021) Improved prime editors enable pathogenic allele correction and cancer modelling in adult mice. *Nat. Commun.* 12, 2121
49. Wang, L. *et al.* (2021) Spelling changes and fluorescent tagging with prime editing vectors for plants. *Front. Genome Ed.* 3, 617553
50. Lin, Q. *et al.* (2020) Prime genome editing in rice and wheat. *Nat. Biotechnol.* 38, 582–585
51. Jiang, Y.Y. *et al.* (2020) Prime editing efficiently generates W542L and S621I double mutations in two ALS genes in maize. *Genome Biol.* 21, 257
52. Lu, Y. *et al.* (2021) Precise genome modification in tomato using an improved prime editing system. *Plant Biotechnol. J.* 19, 415–417
53. Lin, Q. *et al.* (2021) High-efficiency prime editing with optimized, paired pegRNAs in plants. *Nat. Biotechnol.* 39, 923–927
54. Kim, H.K. *et al.* (2021) Predicting the efficiency of prime editing guide RNAs in human cells. *Nat. Biotechnol.* 39, 198–206
55. Arezi, B. and Hogrefe, H. (2009) Novel mutations in Moloney murine leukemia virus reverse transcriptase increase thermostability through tighter binding to template-primer. *Nucleic Acids Res.* 37, 473–481
56. Chen, P.J. *et al.* (2021) Enhanced prime editing systems by manipulating cellular determinants of editing outcomes. *Cell* 184, 5635–5652
57. Velimirovic, M. *et al.* (2022) Peptide fusion improves prime editing efficiency. *Nat. Commun.* 13, 3512
58. Zong, Y. *et al.* (2022) An engineered prime editor with enhanced editing efficiency in plants. *Nat. Biotechnol.* 40, 1394–1402
59. Chow, R.D. *et al.* (2021) A web tool for the design of prime-editing guide RNAs. *Nat. Biomed. Eng.* 5, 190–194
60. Hsu, J.Y. *et al.* (2021) PrimeDesign software for rapid and simplified design of prime editing guide RNAs. *Nat. Commun.* 12, 1034
61. Hwang, G.H. *et al.* (2021) PE-Designer and PE-Analyzer: web-based design and analysis tools for CRISPR prime editing. *Nucleic Acids Res.* 49, W499–W504
62. Siegner, S.M. *et al.* (2021) PnB Designer: a web application to design prime and base editor guide RNAs for animals and plants. *BMC Bioinformatics* 22, 101
63. Anderson, M.V. *et al.* (2021) pegIT – a web-based design tool for prime editing. *Nucleic Acids Res.* 49, W505–W509
64. Liu, Y. *et al.* (2021) Enhancing prime editing by Csy4-mediated processing of pegRNA. *Cell Res.* 31, 1134–1136
65. Li, X. *et al.* (2022) Highly efficient prime editing by introducing same-sense mutations in pegRNA or stabilizing its structure. *Nat. Commun.* 13, 1669
66. Zhang, G. *et al.* (2022) Enhancement of prime editing via xrRNA motif-joined pegRNA. *Nat. Commun.* 13, 1856
67. Nelson, J.W. *et al.* (2022) Engineered pegRNAs improve prime editing efficiency. *Nat. Biotechnol.* 40, 402–410
68. Choi, J. *et al.* (2022) Precise genomic deletions using paired prime editing. *Nat. Biotechnol.* 40, 218–226
69. Anzalone, A.V. *et al.* (2022) Programmable deletion, replacement, integration and inversion of large DNA sequences with twin prime editing. *Nat. Biotechnol.* 40, 731–740
70. Jiang, T. *et al.* (2022) Deletion and replacement of long genomic sequences using prime editing. *Nat. Biotechnol.* 40, 227–234
71. Tao, R. *et al.* (2022) Bi-PE: bi-directional priming improves CRISPR/Cas9 prime editing in mammalian cells. *Nucleic Acids Res.* 50, 6423–6434
72. Wang, J. *et al.* (2022) Efficient targeted insertion of large DNA fragments without DNA donors. *Nat. Methods* 19, 331–340
73. Ferreira da Silva, J. *et al.* (2022) Prime editing efficiency and fidelity are enhanced in the absence of mismatch repair. *Nat. Commun.* 13, 760
74. Kleinstiver, B.P. *et al.* (2015) Engineered CRISPR–Cas9 nucleases with altered PAM specificities. *Nature* 523, 481–485
75. Hu, J.H. *et al.* (2018) Evolved Cas9 variants with broad PAM compatibility and high DNA specificity. *Nature* 556, 57–63
76. Nishimasu, H. *et al.* (2018) Engineered CRISPR–Cas9 nuclease with expanded targeting space. *Science* 361, 1259–1262
77. Kweon, J. *et al.* (2021) Engineered prime editors with PAM flexibility. *Mol. Ther.* 29, 2001–2007
78. Wu, Z. *et al.* (2006) Adeno-associated virus serotypes: vector toolkit for human gene therapy. *Mol. Ther.* 14, 316–327
79. Zhi, S. *et al.* (2022) Dual-AAV delivering split prime editor system for in vivo genome editing. *Mol. Ther.* 30, 283–294
80. Liu, B. *et al.* (2022) A split prime editor with untethered reverse transcriptase and circular RNA template. *Nat. Biotechnol.* 40, 1388–1393
81. Doudna, J.A. (2020) The promise and challenge of therapeutic genome editing. *Nature* 578, 229–236
82. Chemello, F. *et al.* (2021) Precise correction of Duchenne muscular dystrophy exon deletion mutations by base and prime editing. *Sci. Adv.* 7, eabg4910
83. Jang, H. *et al.* (2022) Application of prime editing to the correction of mutations and phenotypes in adult mice with liver and eye diseases. *Nat. Biomed. Eng.* 6, 181–194
84. Shedlovsky, A. *et al.* (1993) Mouse models of human phenylketonuria. *Genetics* 134, 1205–1210
85. Aulicino, F. *et al.* (2022) Highly efficient CRISPR-mediated large DNA docking and multiplexed prime editing using a single baculovirus. *Nucleic Acids Res.* 50, 7783–7799
86. Li, H. *et al.* (2022) Multiplex precision gene editing by a surrogate prime editor in rice. *Mol. Plant* 15, 1077–1080
87. Torkamani, A. *et al.* (2018) The personal and clinical utility of polygenic risk scores. *Nat. Rev. Genet.* 19, 581–590
88. Wrona, D. *et al.* (2020) CRISPR-directed therapeutic correction at the NCF1 locus is challenged by frequent incidence of chromosomal deletions. *Mol. Ther. Methods Clin. Dev.* 17, 936–943
89. Asmamaw Mengstie, M. (2022) Viral vectors for the in vivo delivery of CRISPR components: advances and challenges. *Front. Bioeng. Biotechnol.* 10, 895713
90. Taha, E.A. *et al.* (2022) Delivery of CRISPR–Cas tools for in vivo genome editing therapy: trends and challenges. *J. Control. Release* 342, 345–361
91. Kazemian, P. *et al.* (2022) Lipid-nanoparticle-based delivery of CRISPR/Cas9 genome-editing components. *Mol. Pharm.* 19, 1669–1686
92. D'Astolfo, D.S. *et al.* (2015) Efficient intracellular delivery of native proteins. *Cell* 161, 674–690
93. Staahl, B.T. *et al.* (2017) Efficient genome editing in the mouse brain by local delivery of engineered Cas9 ribonucleoprotein complexes. *Nat. Biotechnol.* 35, 431–434
94. Raguram, A. *et al.* (2022) Therapeutic in vivo delivery of gene editing agents. *Cell* 185, 2806–2827
95. Lino, C.A. *et al.* (2018) Delivering CRISPR: a review of the challenges and approaches. *Drug Delivery* 25, 1234–1257
96. Verdera, H.C. *et al.* (2020) AAV vector immunogenicity in humans: a long journey to successful gene transfer. *Mol. Ther.* 28, 723–746
97. Asmamaw, M. and Zawdie, B. (2021) Mechanism and applications of CRISPR/Cas-9-mediated genome editing. *Biologics: Targets Ther.* 15, 353
98. Chen, S. *et al.* (2016) Highly efficient mouse genome editing by CRISPR ribonucleoprotein electroporation of zygotes. *J. Biol. Chem.* 291, 14457–14467
99. Yin, H. *et al.* (2016) Therapeutic genome editing by combined viral and non-viral delivery of CRISPR system components in vivo. *Nat. Biotechnol.* 34, 328–333
100. Zuris, J.A. *et al.* (2015) Cationic lipid-mediated delivery of proteins enables efficient protein-based genome editing in vitro and in vivo. *Nat. Biotechnol.* 33, 73–80
101. Ramakrishna, S. *et al.* (2014) Gene disruption by cell-penetrating peptide-mediated delivery of Cas9 protein and guide RNA. *Genome Res.* 24, 1020–1027
102. Gori, J.L. *et al.* (2015) Delivery and specificity of CRISPR/Cas9 genome editing technologies for human gene therapy. *Hum. Gene Ther.* 26, 443–451
103. Yang, H. *et al.* (2013) One-step generation of mice carrying reporter and conditional alleles by CRISPR/Cas-mediated genome engineering. *Cell* 154, 1370–1379
104. Lyu, P. *et al.* (2020) Virus-like particle mediated CRISPR/Cas9 delivery for efficient and safe genome editing. *Life* 10, 366
105. Larrea, A.A. *et al.* (2010) SnapShot: DNA mismatch repair. *Cell* 141, 730–731
106. Iyer, R.R. *et al.* (2006) DNA mismatch repair: functions and mechanisms. *Chem. Rev.* 106, 302–323

107. Kunkel, T.A. and Erie, D.A. (2005) DNA mismatch repair. *Annu. Rev. Biochem.* 74, 681–710
108. Li, G.-M. (2008) Mechanisms and functions of DNA mismatch repair. *Cell Res.* 18, 85–98
109. Gupta, S. *et al.* (2012) Mechanism of mismatch recognition revealed by human MutSβ bound to unpaired DNA loops. *Nat. Struct. Mol. Biol.* 19, 72–78
110. Warren, J.J. *et al.* (2007) Structure of the human MutSα DNA lesion recognition complex. *Mol. Cell* 26, 579–592
111. Kadyrov, F.A. *et al.* (2006) Endonucleolytic function of MutLα in human mismatch repair. *Cell* 126, 297–308
112. Pluciennik, A. *et al.* (2010) PCNA function in the activation and strand direction of MutLα endonuclease in mismatch repair. *Proc. Natl. Acad. Sci. U. S. A.* 107, 16066–16071
113. Genschel, J. *et al.* (2002) Human exonuclease I is required for 5′ and 3′ mismatch repair. *J. Biol. Chem.* 277, 13302–13311
114. Zhang, Y. *et al.* (2005) Reconstitution of 5′-directed human mismatch repair in a purified system. *Cell* 122, 693–705